Case Study

Effect of Soil-Foundation Interaction on the Dynamic Response of a Four-Cylinder Compressor Foundation

O. S. Ali, Ph.D., P.E., M.ASCE[1]; and Mustafa Mahamid, Ph.D., P.E., S.E., F.ASCE[2]

Abstract: The dynamic response of a machine-foundation system depends on several factors, such as (1) the soil dynamic properties, (2) geometric properties of the foundation, (3) amplitude of the applied dynamic loads, and (4) frequency of the dynamic excitation force. The main goal in machine foundation design is to keep the foundation response within a specific limit to enable the satisfactory operation of the machine. If the foundation response exceeds this limit, the foundation will adversely affect the performance of the machine and may damage the machine internals or cause it to function improperly. Furthermore, the excessive vibrations impose additional stresses on the machine resulting in increased unbalanced loading, and thus, to increased dynamic loads on the soil-foundation system. This paper presents the results of the dynamic analysis of a four-cylinder compressor foundation. The original design of the foundation was performed in the early 1960s and ignored the effect of the soil on the response of the foundation system; therefore, the foundation has been suffering from excessive loading. The foundation block supported a four-cylinder compressor, suction and discharge bottles, and a crank and driving motor with a total weight of approximately 974 kN (219 kips). The results of a three-dimensional (3D) finite-element model of a soil-foundation system was used to determine the dynamic response of the soil-foundation system and to assess the foundation response under applied dynamic loading resulting from the compressor crank. The dynamic analysis was performed by performing (1) eigenvalue analysis of the foundation block, considering the effect of the soil-foundation interaction, to determine the soil-foundation natural frequencies and modal participation factors and (2) a forced response of the foundation under an unbalanced crankshaft load applied to determine the forced response amplitude of the soil-foundation system. **DOI: 10.1061/(ASCE)SC.1943-5576.0000380.** © *2018 American Society of Civil Engineers.*

Author keywords: Compressor foundation; Soil-structure interaction; Finite-element method; Dynamic loading; Machine foundation; Stiffness; Damping.

Introduction

Large reciprocating compressors are used in a number of industries, including those of gas, oil, and petrochemical production. The foundation supporting the compressor equipment is subject to high vibrations instigated by the unbalanced machine forces and the machine operating speed. Therefore, for the compressor to show satisfactory operation, the vibrations (dynamic amplitude) of the machine resulting from these dynamic forces should be limited to very small values at the location of the machine anchorage to the foundation. Usually these limits do not exceed a few micrometers (10–12 μm). If the dynamic amplitude at the machine bearings exceeded such limits, excessive vibrations occurred and damaged the machine or caused it to function improperly. Furthermore, these vibrations adversely affected the building or people working near the machinery unless the frequency and amplitude of the vibrations were controlled. Therefore, to limit the vibrational amplitudes generated by these machines, reciprocating compressor foundations were normally built as massive solid concrete blocks doweled to a single mat or to a continuous mat supporting several machines. Depending on the soil properties, the foundation mat was supported directly, either by the soil continuum or by piles. The design of these foundations was often conducted using a rule of thumb indicating that increasing the weight of the foundation and/or strengthening the soil beneath the foundation base provides highly tuned supports for the machine. The total weight of this kind of foundation design was usually maintained at 2–3 times the weight of the machine it supported. It was not until the 1950s that the vibration analysis of the machine foundations was implemented using the lumped mass approach and was based on a theory of a surface load on an elastic half-space. The theory of the elastic half-space assumed that the foundation was (1) on the surface of a homogeneous stratum overlaying the bedrock and (2) partially consisting of fully embedded foundations in a homogeneous stratum overlaying the bedrock. Theory of the elastic half-space ignored the shape of the foundation and assumed that the foundation had a circular contact base. The effect of the foundation geometry was later considered by Kobori (1962), who determined the dynamic amplitude response in the vertical, lateral, and rocking modes of vibration for a rectangular foundation. Chae (1969) suggested the use of equivalent radii to estimate the response of the rectangular foundation.

The quality of the design and construction of the compressor mounting system and the integrity of the foundation for the reciprocating compressor foundation affected long-term operation reliability. Degradation of the soil-foundation system resulted in additional differential displacement of the foundation, resulting in misalignment of the compressor shaft and an increase in the unbalanced loading on the foundation; thus, it increased the foundation

[1]Manager of Engineering, Structural Technologies, Inc., 10150 Old Columbia Rd., Columbia, MD 19806. E-mail: osali@structuraltec.com

[2]Clinical Associate Professor, Univ. of Illinois at Chicago, Chicago, IL 60607-7023 (corresponding author). E-mail: mmahamid@uic.edu

Note. This manuscript was submitted on October 25, 2017; approved on January 10, 2018; published online on May 3, 2018. Discussion period open until October 3, 2018; separate discussions must be submitted for individual papers. This paper is part of the ***Practice Periodical on Structural Design and Construction***, © ASCE, ISSN 1084-0680.

vibration and eventually crankshaft failure. A sound design for the compressor foundation not only could accommodate all applied loads, including the horizontal, gas, and inertia loads, the compressor and foundation weights, the thermal loading, and the compressor frame distortion, but it could also reduce the effects of the vibration on the foundation and the soil as well.

Because of the complexity of the analysis to mitigate the effect of negative vibrations on the compressor foundation and the interaction of the foundation with the soil response, a finite-element tool was usually used to perform an analysis and design the foundation. Because the finite-element modeling was a numerical representation of a physical engineering system, the model could accurately capture the geometric details of the system, the actual boundary conditions, and the excitation environment of the dynamic system to simulate the real behavior of the problem. Generally, a dynamic finite-element analysis consisted of three major steps: (1) idealization of the geometry, materials, and loading; (2) formulation of the stiffness, mass, and damping matrices; and (3) solutions for the resulting equations of motion. A fundamental kinematic assumption of all FEMs was that the displacement field $u(x,y)$ was completely defined by the displacement vector $[u]$ of the nodal points of the system. Several parameters affected the finite-element results of the model, such as the element type, element size, boundary conditions, and the effect of the soil-structure interaction on the response of the machine-foundation system. During machine oscillation, the machine-foundation system interacted with the soil through two mechanisms that occurred simultaneously with a minor time lag:

1. Kinematic interaction, which was the difference in motion of the foundation system and the free-field motion due to the presence of the stiff foundation system, waves inclination, waves incoherence, and foundation embedment; and
2. Inertial interaction, which was the additional inertial dynamic forces and displacements that were imposed on the soil-foundation system during machine-foundation oscillation.

Both kinds of interaction must be considered in the machine-foundation system to achieve the proper design. While some researchers think that ignoring the effect of the foundation-structure interaction (SSI) was conservative, Kavvads and Gazetas (1993) suggested that the effect of the SSI increased the structural demands, and the forces that resulted from the SSI governed the structural response. These forces were determined with accurate analyses.

This paper presents an investigation into the dynamic response of a four-cylinder Dress-Rand compressor (Washington, DC) foundation considering the effect of the soil-structure interaction on the dynamic response of the foundation. The dynamic analysis of the foundation was performed to evaluate the foundation response under applied dynamic loading resulting from the compressor crank. The dynamic analysis was conducted by performing (1) an eigenvalue analysis of the foundation block considering the effect of the soil-foundation interaction to determine the soil-foundation natural frequencies and the modal participation factors and (2) forced-response analysis of the foundation under an unbalanced crank load applied to determine the forced response amplitude of the soil-foundation system.

Foundation Geometry

The foundation block supported a four-cylinder Dress-Rand compressor, suction and discharge bottles, and a crank driving motor with a total weight of approximately 974 kN (219 kips). Figs. 1 and 2 show the plan and section views of the foundation block.

Design Input

Soil Data

The main design input parameters affecting the computation of the soil dynamic springs were presented in the soil geotechnical report provided by the geotechnical engineer who investigated the site and the foundation presented in this study.

Soil shear wave velocity:

$$V_s = 201\,\text{m/s}\,(V_s = 7{,}913\,\text{in./s}) \tag{1}$$

Soil compression wave velocity:

$$V_p = 1{,}440\,\text{m/s}\,\left(V_p = 56{,}693\,\text{in./s}\right) \tag{2}$$

Soil mass density:

$$r = 2.00\,\text{g/cm}^3\,\left(r = 0.072\,\text{lb/in.}^3\right) \tag{3}$$

On the basis of the soil shear and compression wave velocities, the soil dynamic properties are calculated as

Soil Poisson's ratio:

$$\nu = \left[V_p^2 + 2\cdot V_s^2\right] / \left[2\cdot\left(V_p^2 - V_s^2\right)\right] \tag{4}$$

Soil dynamic shear modulus:

$$G_{\text{dynamic}} = \rho\cdot V_s \tag{5}$$

Soil dynamic Young's modulus :

$$E_{\text{soil}} = 2\cdot\rho\cdot V_s^2(1+\nu) \tag{6}$$

The effect of the soil layering on the foundation was a complex phenomenon, and the soil stiffness and damping were highly dependent on the soil shear modulus and the forcing frequency of the excitation. To determine the soil stiffness and damping coefficients, the weighted average shear modulus is evaluated according to the elastic half-space theory as follows:

$$G_{\text{soil}} = \left(\sum_{i=1}^{n}\frac{h_i}{A_i}\right) / \left(\sum_{i=1}^{n}\frac{h_i}{A_i\cdot G_i}\right) \tag{7}$$

where h_i = thickness of the ith soil layer; G_i = shear modulus of the ith soil layer; A_i = area of stress influence of a horizontal plane (spreading below the foundation at a ratio of 2:1) measured at the center of ith soil layer; and n = number of soil layers to a depth equal to one diameter or one long dimension of the foundation, whichever is greater.

Machine Data

The weights of the compressor assembly components used in the analysis are as listed in Table 1.

Concrete Properties

The material properties of a member used in the finite-element model were based on the steel properties of the steel framing and

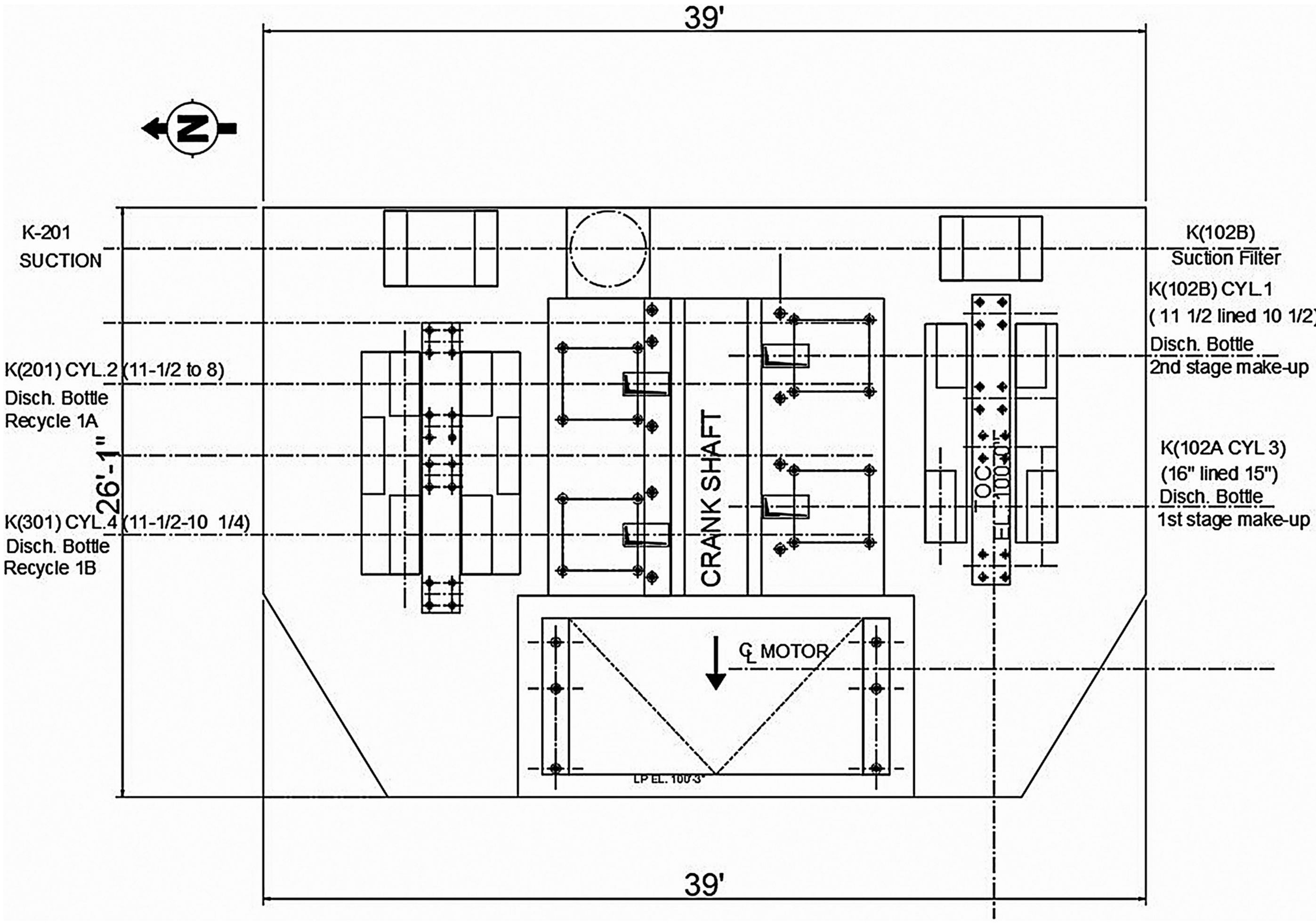

Fig. 1. Compressor foundation plan view

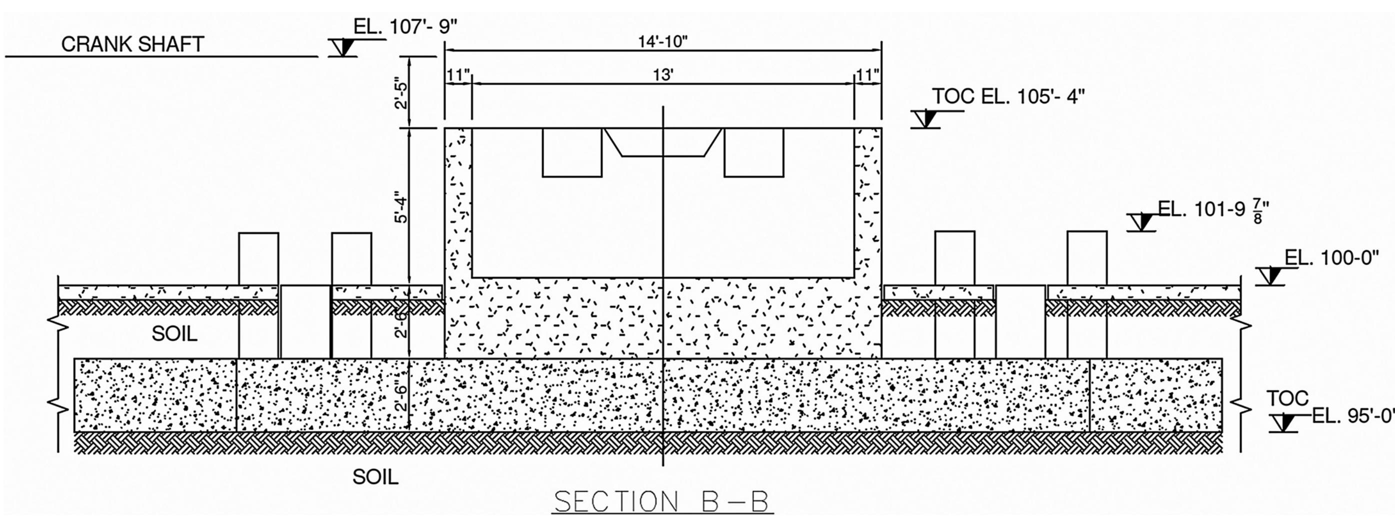

Fig. 2. Compressor foundation section view

the concrete compressive strength. The material properties for the foundation-base mat shell elements and the foundation piers are calculated as

Concrete Young's modulus :

$$E_c = 4,700\sqrt{f_c} \ \ (\text{MPa}) \times \left[E_c = 57,000\sqrt{f_c}(\text{psi})\right] \tag{8}$$

where f_c = concrete compressive strength of 20.684 MPa (3,000 psi) based on the American Concrete Institute (ACI) standard ACI 318-11 used for the calculation (ACI 2011).

Table 1. Weight of the Compressor Components Assembly

Weight	Value
Motor rotor $\{Wt_{\text{mot}}[\text{kN(kip)}]\}$	79 (17.8)
Running gear $\{Wt_{\text{gear}}[\text{kN(kip)}]\}$	667 (150)
Cylinders $\{Wt_{\text{cyl}}\ [\text{kN(kip)}]\}$	80 (18)
Suction bottles $\{Wt_{\text{scu}}[\text{kN(kip)}]\}$	27.5 (6.2)
Recycle bottle $\{Wt_{\text{rec}}[\text{kN(kip)}]\}$	33.4 (7.5)
Motor stator and other density parts $\{Wt_{\text{mot}}[\text{kN(kip)}]\}$	91.6 (20.6)
Discharge bottles $\{Wt_{\text{dis}}[\text{kN(kip)}]\}$	42.3 (9.52)

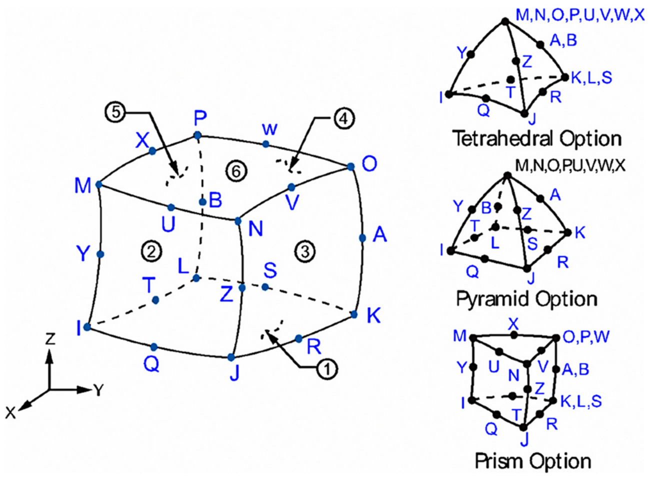

Fig. 3. SOLID186 structural element

$$\text{Concrete shear modulus} : G_s = \frac{E_c}{2 \cdot (1 + \nu)} \tag{9}$$

where ν = Poisson's ratio for concrete is equal to 0.17.

Modeling of the Soil-Foundation System

To determine the dynamic properties of the soil-foundation system, a three-dimensional (3D) finite-element model was created using the finite-element code of *ANSYS 13*. The soil continuum was modeled using the *ANSYS 13* 3D brick element SOLID186. The *ANSYS 13* element SOLID186 was a 3D 20-noded solid element that exhibited quadratic displacement behavior. The element was defined by 20 nodes that each had three degrees of freedom (DOF) per node, which are translations in the nodal x-, y-, and z-directions. The SOLID186 structural solid was suitable for modeling general 3D solid structures because it allowed for prism, tetrahedral, and pyramid degenerations when used in irregular regions. The default *ANSYS 13* KEYOPT values were selected to control the behavior of the element. Fig. 3 shows the geometry of the SOLID 186 element used for the finite-element analysis.

The running time and accuracy of a finite-element solution were greatly affected by the mesh quality; in other words, they were affected by the element type, size, shape, and aspect ratio used during the modeling stage. Several recommendations were provided in the literature to set the element size for wave propagation analyses using a FEM. The general concept was that the mesh should be fine enough to resolve the propagating wave. Overall, the recommendations provided in the literature suggest a range between 5 and 20 elements per wavelength. The size, S_e, of the elements was chosen on the basis of the recommendation of Lysmer and Kuhlemeyer (1969) such that the size of the elements was based on the maximum frequency content of the applied loads. Lysmer and Kuhlemeyer

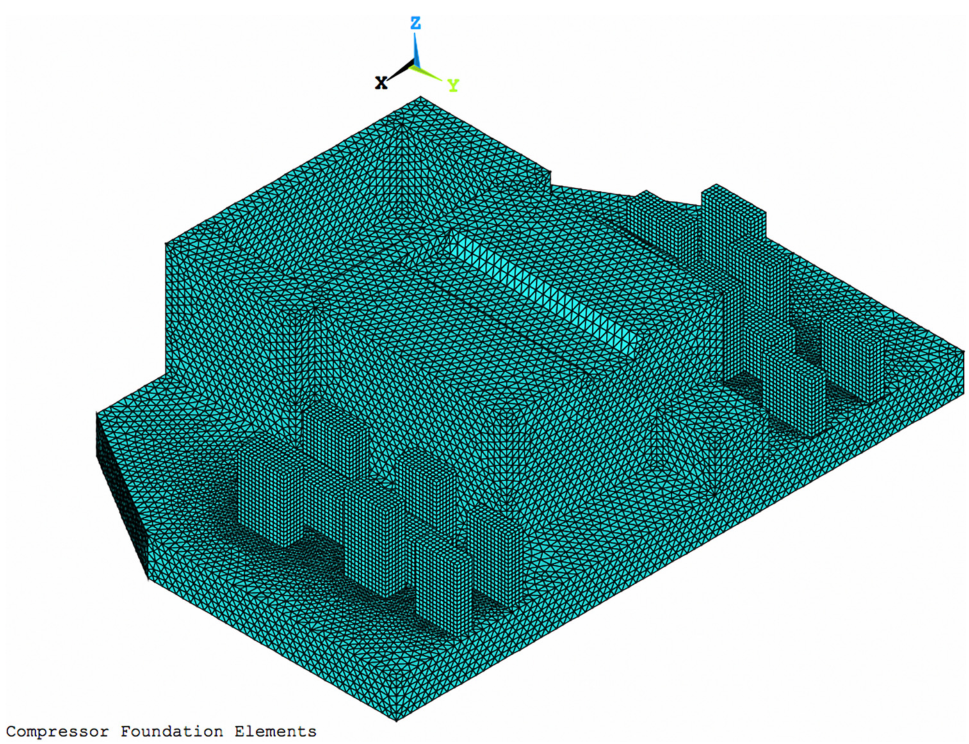

Fig. 4. Compressor foundation finite-element model

(1969) proposed the following criteria for selecting the finite-element size:

$$S_e \approx 0.2\lambda_{\text{shear}} \tag{10}$$

where S_e = finite-element size; and λ_{shear} = soil shear wavelength (in meters).

Fig. 4 shows the finite-element model (discretized model) of the compressor foundation.

The flexibility of the soil-supporting media was incorporated in the analysis by considering the translational springs in the three orthogonal directions attached at the base mat finite-element nodes. The effect of the soil on the response of the compressor foundation was captured by modeling the soil dynamic elastic properties using spring-damper elements. *ANSYS 13* element COMBIN14 was used to model the vertical and lateral stiffness of the soil, as shown in Fig. 5. The element had longitudinal or torsional capability. The longitudinal spring-damper option was a uniaxial tension-compression element with as many as three DOF at each node, which are translations in the nodal x-, y-, and z-directions.

The element was defined by two nodes: a spring constant, K, and damping coefficient, Cv.

The longitudinal spring-element constant had a unit of force/length; the damping coefficient unit was in force time/length. The element behavior was controlled using the element KEY OPTIONS. The vertical and lateral spring constants assigned to the soil spring elements are determined based on the following relationships:

$$K_{\text{lateral}} = (K_{hd}) \cdot A_{\text{joint}} \tag{11}$$

$$K_{\text{vertical}} = (K_{vd}) \cdot A_{\text{joint}} \tag{12}$$

where K_{lateral} and K_{vertical} = global lateral and vertical dynamic spring stiffness of the soil, in kN per cubic meter (kip per cubic feet); A_{joint} = area served by each joint of the base mat elements. In the analysis of the structural elements supported by the soil, modeling could be performed in one of several methods. One method was by modeling the soil with a 3D solid element, which would require that all the soil properties be put into the model; however, obtaining all soil properties required for modeling could be challenging sometimes. Another method was by modeling the soil using spring elements, which would require that the spring stiffnesses be put into the model. The spring elements were created at a node, and each node could serve the tributary area, A_{joint}, of that specific node. In this analysis, spring elements were used because they are accurate and relatively easy to model using the spring stiffness equations identified in the following paragraph.

The lateral and vertical global dynamic stiffnesses of the soil were evaluated on the basis of the elastic half-space theory considering the effect the foundation embedment on the soil stiffness and damping constant. The global lateral and vertical stiffnesses of the soil are calculated per Arya et al. (1984) in Eqs. (13) and (14), respectively, as follows:

$$K_{hd} = 2 \cdot (1 + \upsilon) \cdot G_{\text{soil}} \cdot \beta_h \cdot \sqrt{B \cdot L} \cdot \eta_h \tag{13}$$

$$K_{vd} = \frac{G_{\text{soil}}}{(1 - \nu)} \cdot \beta_z \cdot \sqrt{B \cdot L} \cdot \eta_z \tag{14}$$

where ν = soil Poisson's ratio; G_{soil} = soil shear modulus; β_h = foundation geometric factors; B and L = foundation width and length, respectively; and η_h = foundation embedment factor for the lateral mode of vibration obtained, as follows, from Arya et al. (1984):

$$\eta_h = 1 + 0.55 \cdot (2 - \upsilon) \cdot \frac{h_{\text{soil}}}{R_{\text{eqv}}} \tag{15}$$

η_z is the foundation embedment factor for the vertical mode of vibration obtained from Arya et al. (1984) as follows:

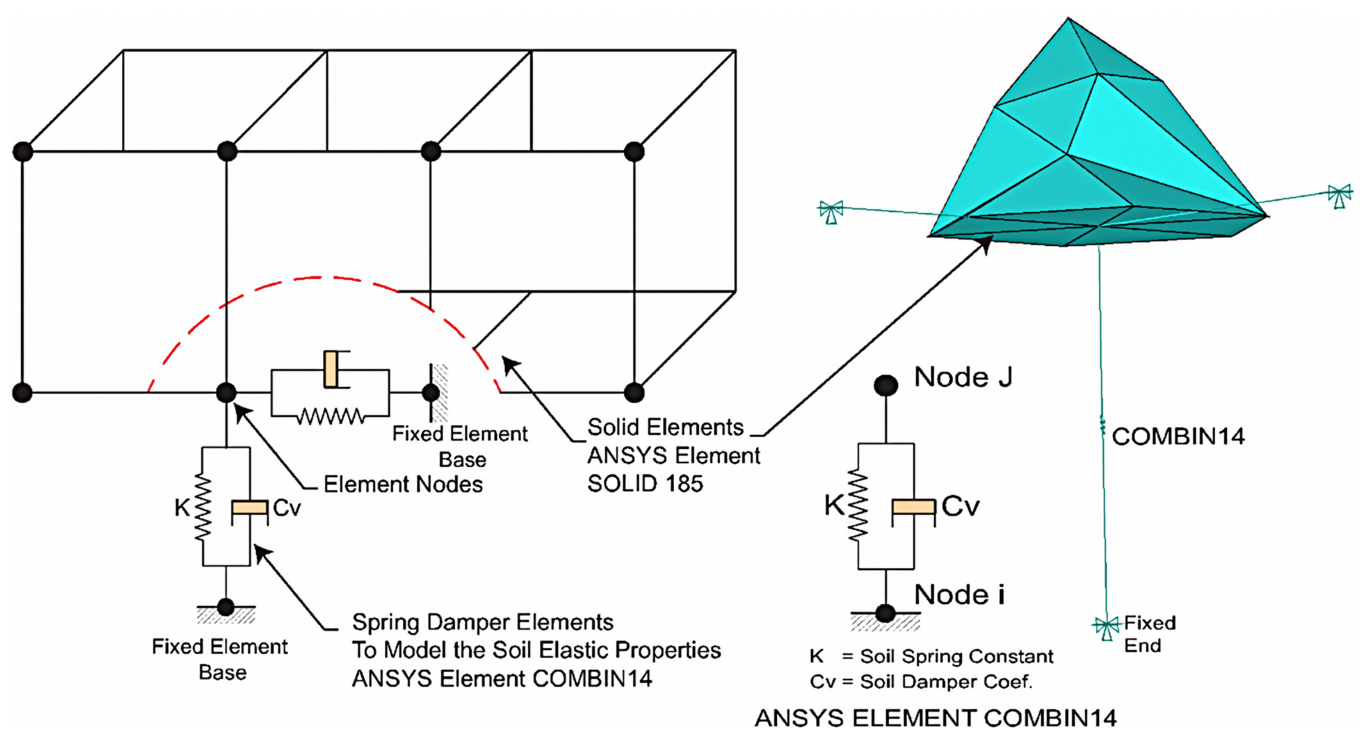

Fig. 5. Spring-damper element

$$\eta_z = 1 + 0.6 \cdot (1 - \upsilon) \cdot \frac{h_{\text{soil}}}{R_{\text{eqv}}} \tag{16}$$

where h_{soil} = foundation embedment depth; and R_{eqv} = foundation equivalent radius.

To capture the effect of the equipment weight on the foundation dynamic response, the masses of the crank, cylinder, and the motor were added to the model in the form of masses lumped at the component support plate. *ANSYS 13* element type MASS21 was used to model the component masses. MASS21 was a point element having as many as six DOF, which were translations in the nodal *x*-, *y*-, and *z*-directions and rotations about the nodal *x*-, *y*-, and *z*-axes. A different mass and rotary inertia was assigned to each coordinate direction. The mass element was defined by a single node and the concentrated mass components (force × time^2/length) were in the element coordinate directions. The element coordinate system was set parallel to the global Cartesian coordinate system. The masses were determined on the basis of the component weights and the area of the sole supporting plate.

Modal Analysis of the Soil-Foundation System

To determine the foundation vibration characteristics, modal analysis was performed using the finite-element model described in the previous section. To determine the fundamental natural frequencies of the foundation and the corresponding modal mass participation factors, the equation of motion for an undamped system is expressed as follows:

$$\mathbf{M}\frac{d^2}{dt^2}[U] + \mathbf{M}[U] = 0 \tag{17}$$

where $\mathbf{M}$ = structure mass matrix; and $[U]$ = displacement vector $[\phi_i] \cdot \cos(w_i t)$, for which $[\phi_i]$ is the eigenvector representing the mode shape of the ith frequency and ω_i is the ith natural circular frequency (in radians per second).

Table 2. Frequencies at Current Lanczoz Cycle

Mode	Frequency (Hz)
1	12.44
2	12.53
3	14.89
4	15.23
5	15.62
6	15.66
7	22.35
8	24.44
9	30.75
13	33.88
14	34.93
15	35.05
16	35.98
17	36.83
18	37.80
19	38.47
20	39.43
21	42.09
22	43.06
23	43.27
24	45.09
25	48.93
26	49.09
27	51.03

Table 3. Participation Factor Calculation for the *x*-Direction

Mode	Frequency (Hz)	Period (S)	Participation factor	Ratio
1	12.4446	0.0804	4.3558	0.057232
2	12.5321	0.0798	2.0848	0.027393
3	14.8916	0.0672	27.482	0.361087
4	15.231	0.0657	11.478	0.15081
5	15.6242	0.0640	−76.108	1
6	15.6641	0.0638	−27.81	0.365408
7	22.3536	0.0447	−2.2159	0.029115
8	24.4395	0.0409	−0.64476	0.008472
9	30.7517	0.0325	−1.7312	0.022746
10	30.9195	0.0323	2.12E-04	0.000003
11	31.9241	0.0313	0.4343	0.005706
12	32.5802	0.0307	−0.30677	0.004031
13	33.8849	0.0295	−0.33431	0.004393
14	34.9272	0.0286	3.65E-02	0.00048
15	35.0477	0.0285	−0.16054	0.002109
16	35.9775	0.0278	−0.34718	0.004562
17	36.8289	0.0272	−1.7421	0.022889
18	37.7992	0.0265	−0.40175	0.005279
19	38.4719	0.0260	−0.63003	0.008278
20	39.4313	0.0254	−1.4689	0.019301
21	42.0866	0.0238	0.27356	0.003594
22	43.0574	0.0232	0.31432	0.00413
23	43.2669	0.0231	0.22819	0.002998
24	45.0904	0.0222	−0.97528	0.012814
25	48.9339	0.0204	−0.0103	0.000135

Table 4. Participation Factor Calculation for the *y*-Direction

Mode	Frequency (Hz)	Period (S)	Participation factor	Ratio
1	12.4446	0.0804	0.73631	0.007559
2	12.5321	0.0798	1.4668	0.015059
3	14.8916	0.0672	−4.8511	0.049804
4	15.231	0.0657	−2.5323	0.025998
5	15.6242	0.0640	34.064	0.349715
6	15.6641	0.0638	−97.405	1
7	22.3536	0.0447	2.5733	0.026419
8	24.4395	0.0409	−0.21252	0.002182
9	30.7517	0.0325	−0.29608	0.00304
10	30.9195	0.0323	−1.1058	0.011352
11	31.9241	0.0313	−0.51373	0.005274
12	32.5802	0.0307	0.18286	0.001877
13	33.8849	0.0295	−0.11518	0.001183
14	34.9272	0.0286	−0.10846	0.001113
15	35.0477	0.0285	−2.49E-02	0.000256
16	35.9775	0.0278	0.19111	0.001962
17	36.8289	0.0272	−0.20989	0.002155
18	37.7992	0.0265	6.98E-02	0.000716
19	38.4719	0.0260	−0.38409	0.003943
20	39.4313	0.0254	0.19571	0.002009
21	42.0866	0.0238	−0.48803	0.00501
22	43.0574	0.0232	3.87E-02	0.000397
23	43.2669	0.0231	−0.44105	0.004528
24	45.0904	0.0222	0.12674	0.001301
25	48.9339	0.0204	−0.78461	0.008055

Table 5. Participation Factor Calculation for the *z*-Direction

Mode	Frequency (Hz)	Period (S)	Participation factor	Ratio
1	12.4446	0.0804	187.51	1
2	12.5321	0.0798	27.359	0.145911
3	14.8916	0.0672	13.112	0.06993
4	15.231	0.0657	2.2533	0.012017
5	15.6242	0.0640	9.6322	0.05137
6	15.6641	0.0638	2.1951	0.011707
7	22.3536	0.0447	−21.536	0.114857
8	24.4395	0.0409	1.9357	0.010323
9	30.7517	0.0325	1.5529	0.008282
10	30.9195	0.0323	0.30098	0.001605
11	31.9241	0.0313	2.2984	0.012258
12	32.5802	0.0307	−0.96686	0.005156
13	33.8849	0.0295	1.2977	0.006921
14	34.9272	0.0286	0.24579	0.001311
15	35.0477	0.0285	0.46882	0.0025
16	35.9775	0.0278	−1.4136	0.007539
17	36.8289	0.0272	1.004	0.005354
18	37.7992	0.0265	−0.51237	0.002733
19	38.4719	0.0260	0.68887	0.003674
20	39.4313	0.0254	−1.2151	0.00648
21	42.0866	0.0238	0.18023	0.000961
22	43.0574	0.0232	−0.17967	0.000958
23	43.2669	0.0231	0.39394	0.002101
24	45.0904	0.0222	0.75957	0.004051
25	48.9339	0.0204	7.79E-02	0.000415

Tables 2–5 list the fundamental natural modes of the soil-foundation system and the corresponding translational and rotational mass participation factors in the global *x*-, *y*-, and *z*-direction. These listings show that some of the dominant natural frequencies of the soil-foundation system ranged between 12 and 15.6 Hz (Modes 1–6) with significant mass participation factors excited within this range of frequencies. The ACI 351 recommended that the foundation natural frequency fall between −20 and +20% of the compressor operating frequency to avoid resonance between the foundation and the machine (ACI Committee 351 2004). The analysis of the soil-foundation system showed that Modes 1–6 fell within the operating range of the compressor with significant mass contribution to these modes.

Figs. 6 and 7 show the foundation mode shape at the frequency of 12.446 and 12.89 Hz, respectively. Figs. 8 and 9 show the foundation mode shape at the frequency of 15.231 and 15.6242 Hz, respectively.

Harmonic Analysis of the Soil-Foundation System

Because of the presence of unbalanced rotating and reciprocating mass and unbalance periodic inertia, dynamic forces and moments were generated in the foundation at the machine-bearing supports. The unbalanced inertial forces resulted from the acceleration and deceleration of the unbalanced reciprocating masses and by the rotation of the eccentric masses. Fig. 10 shows the kinematics of the compressor piston with a crank

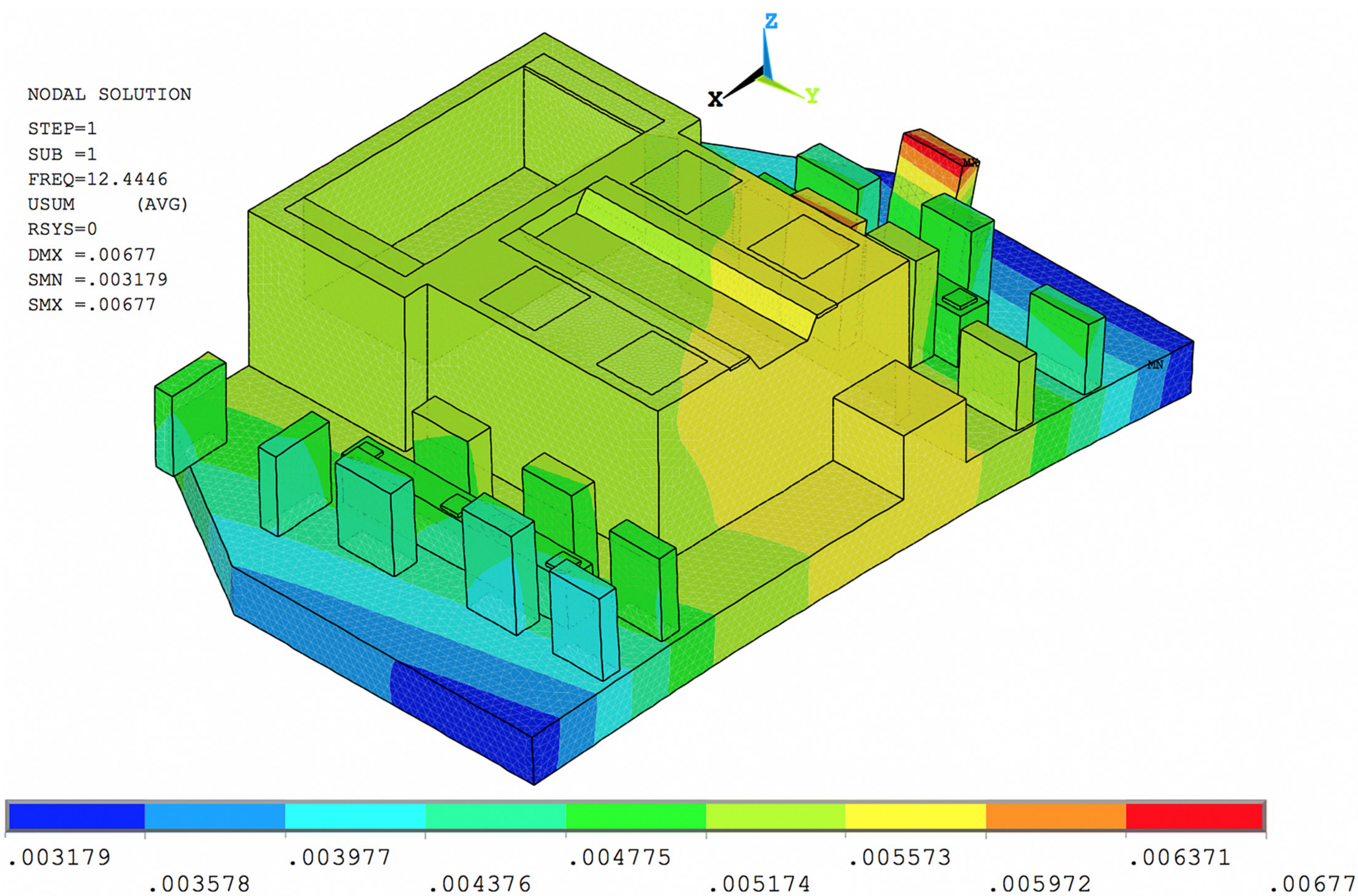

Fig. 6. Foundation mode shape at frequency of 12.446 Hz

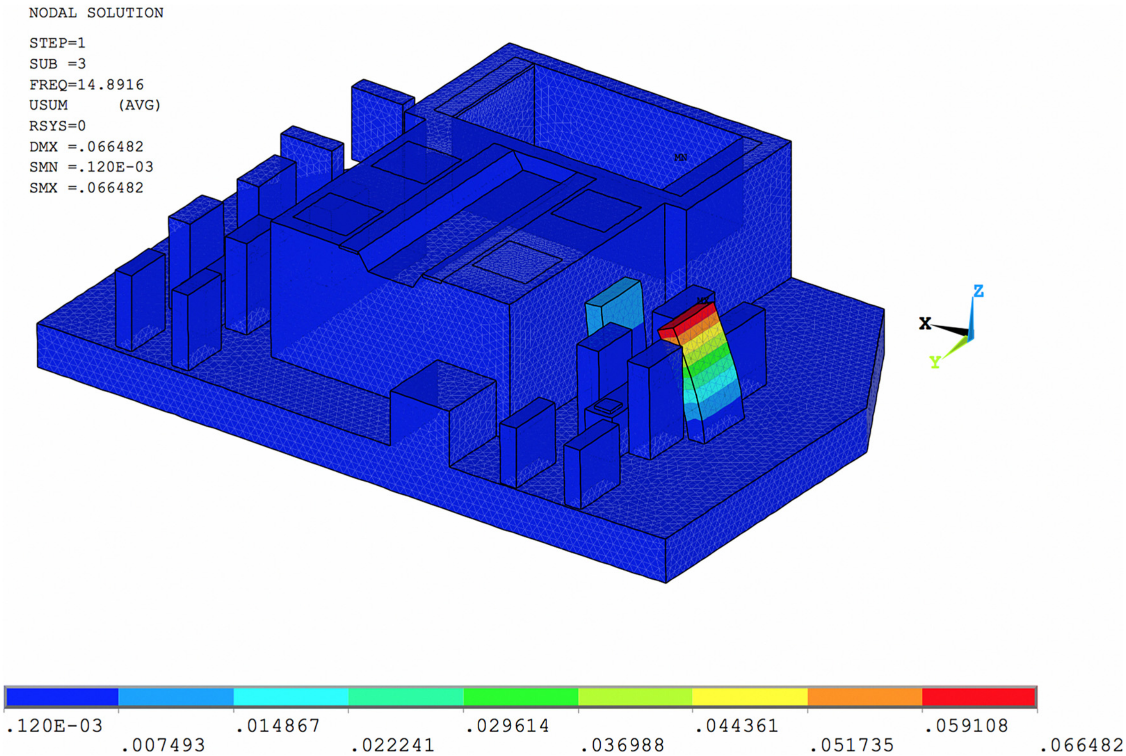

Fig. 7. Foundation mode shape at frequency of 12.89 Hz

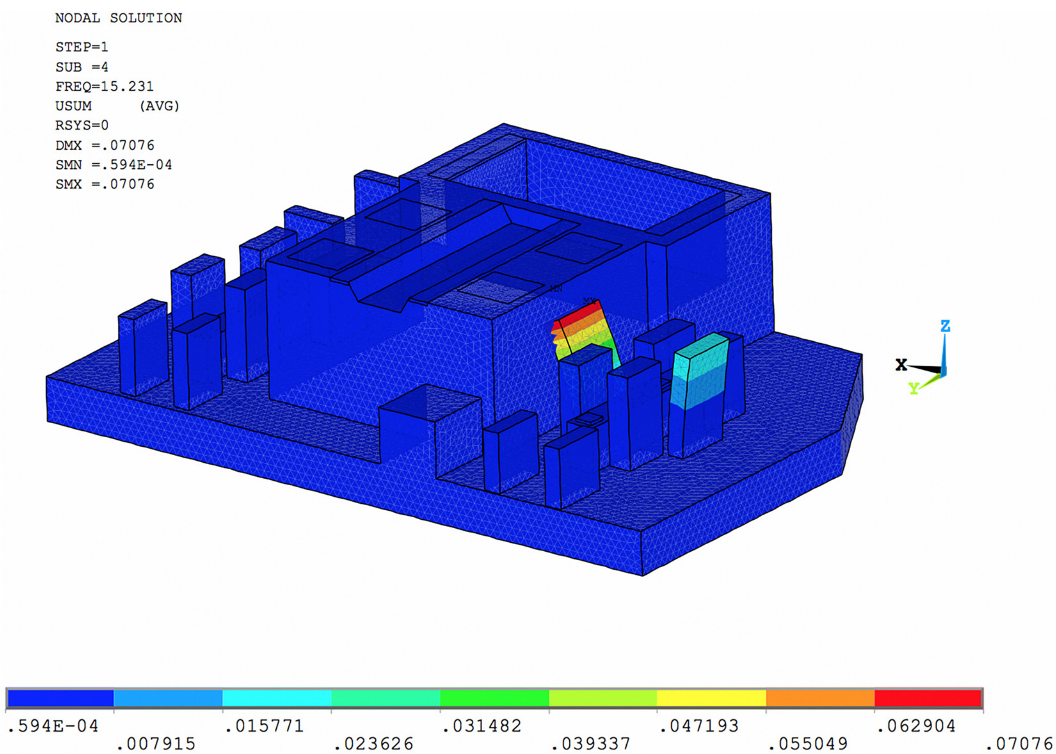

Fig. 8. Foundation mode shape at frequency of 15.231 Hz

counterweight. The rotating masses consisted of the counterweight, crankpin, crankpin web, and approximately one-half of the connecting rod.

The centrifugal forces created by these masses had the same magnitude at all positions of the crank. The resultant unbalanced rotating force is expressed as

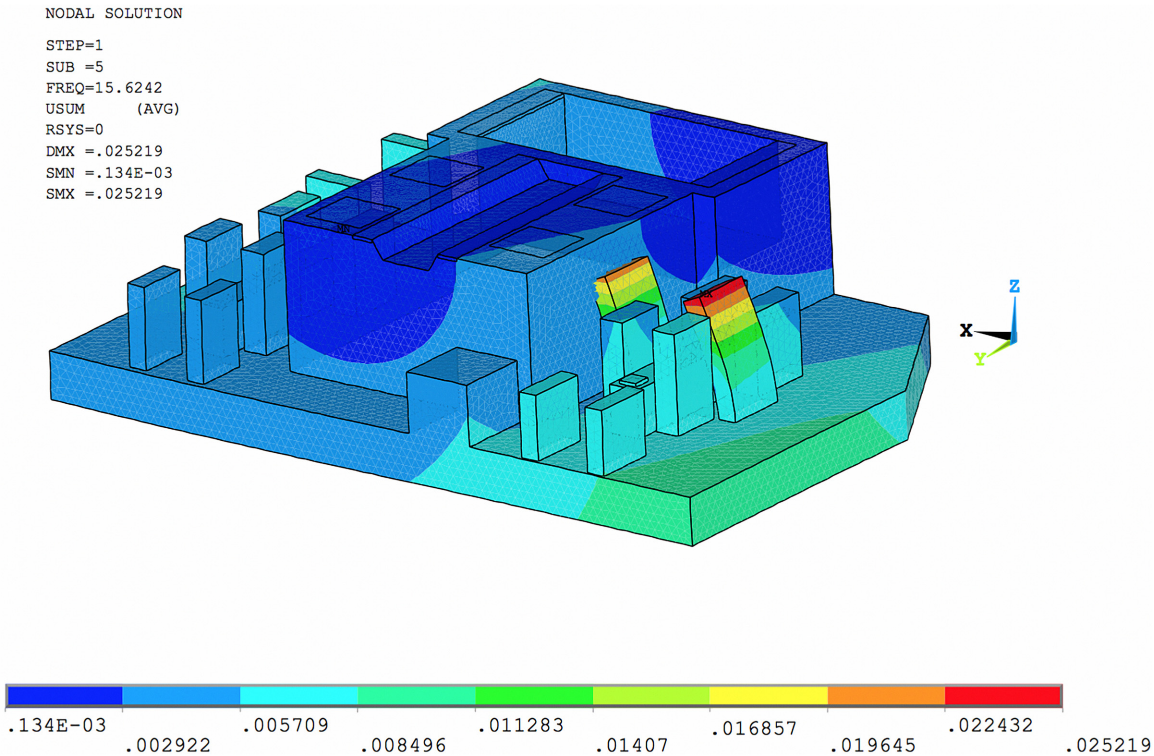

Fig. 9. Foundation mode shape at frequency of 15.6242 Hz

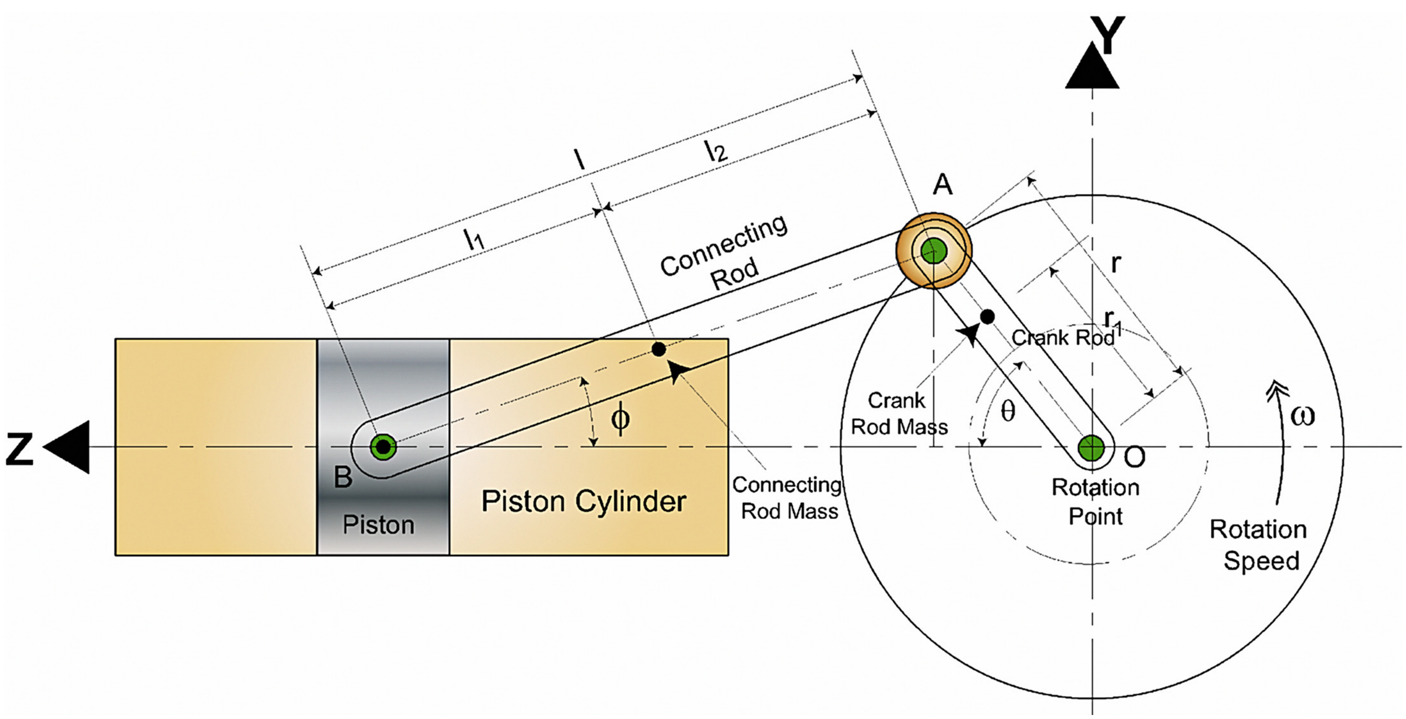

Fig. 10. Kinematics of the compressor cross section

$$F_a = M_a \cdot R \cdot \omega^2 \tag{18}$$

$$M_a = M_r\left(\frac{R_1}{R}\right) + M_c\left(\frac{l_2}{l}\right) \tag{19}$$

where M_r = mass of crank rod; M_c = mass of connecting rod; R = length of crank rod; R_1 = center of gravity of the crank rod from the center of rotation point O; and ω = speed of rotation (in radians per second).

The reciprocating force generated along the axis of the cylinder due to the acceleration of the reciprocating masses of the piston,

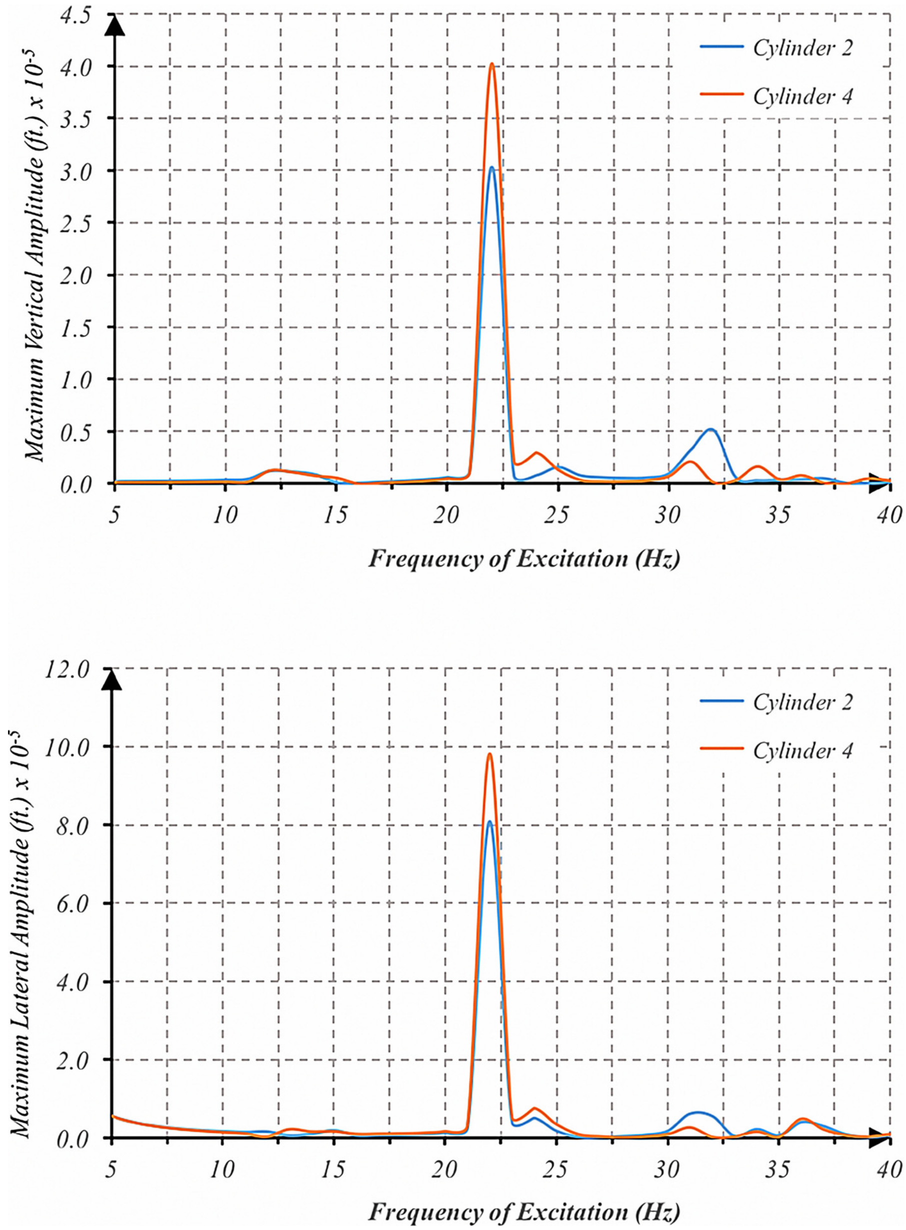

Fig. 11. Harmonic response of Cylinders 2 and 4 supports

piston rod, cross head, and the remaining one half of the connecting rod weight can be expressed as a Fourier series. The acceleration of the reciprocating masses can be expressed with the following Fourier series:

$$F_{\text{piston}} = M_P R \omega^2 \left[\cos(\omega t) + \frac{R}{l} \cdot \cos(2\omega t) \right] \tag{20}$$

where M_p = mass (piston assembly including piston rod, crosshead, etc.); R = length of crank rod; and l = length of the connecting rod.

Figs. 11–13 show the amplitude response of the foundation at different excitation frequencies for the compressor Cylinder 2 and 4 supports, Cylinder 4 discharge bottle support Blocks 1 and 3, suction filter support Blocks 4 and 5; that is, Figs. 11–13 shows the vertical and lateral amplitude responses of the compressor cylinder supports, discharge bottle supports, and suction filter supports at different machine excitation frequencies. Specifically, Fig. 11 shows that the foundation compressor cylinder support was resonating with the machine at an excitation frequency of 23 Hz; Fig. 12 shows that the discharge bottle support blocks were also resonating with the machine at a frequency of 23 Hz, which is within compressor operating frequency; and Fig. 13 shows that the suction filter support was resonating with the machine at 22 Hz in the vertical response and passed through two resonating frequencies, at 15 and 22 Hz, in the lateral direction. Therefore, according to the amplitude responses shown in these figures, the authors concluded that these piers were resonating at the machine operating frequency, and therefore, the configuration of these piers needed to be modified to shift the natural frequency foundation system from the machine operating frequency.

Conclusions

The dynamic assessment of the compressor foundation was determined. A 3D solid block finite-element model was

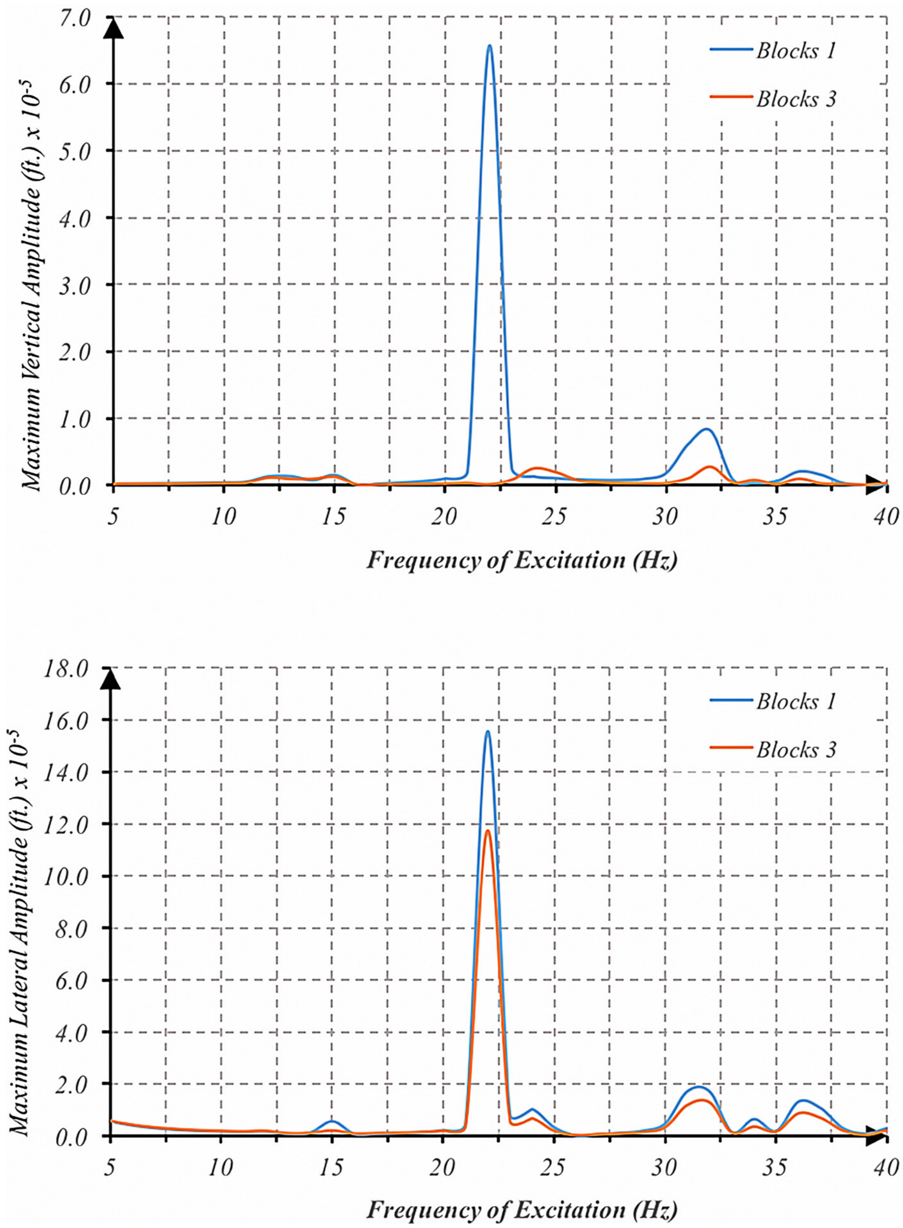

Fig. 12. Harmonic response of Cylinder 4 discharge bottle Supports 1 and 3

developed using the commercial finite-element software. The effect of the soil-foundation interaction was included in the model, in which the soil was modeled as a series of vertical and lateral spring and damper elements. The fundamental natural frequencies and the corresponding mode shapes and mass participation ratios were determined for the soil-foundation system. The response of the soil foundation under forced excitation of unbalanced loading of the machine at different excitation frequencies was calculated and presented. According to the analysis performed, the following conclusions were made:

1. The response of the foundation system was governed by the response of the individual support piers (blocks) and not the global foundation response (i.e., local modes of vibration). The lateral response of the suction filter support pier (Block 4) was excited at a frequency of 12.4 Hz with almost 5% of the foundation mass being excited (mass participation ratio of 5%). This local mode was close to the compressor operation frequency (13.1 Hz).
2. Suction filter support Pier 2 (Block 5) was laterally excited at 15.2 Hz with a mass participation ratio of 0.5%.
3. At a frequency of 15.6 Hz, both the suction filter support piers (Blocks 4 and 5) were laterally excited with 18% of the foundation mass contributing to this mode.
4. Under harmonic excitation (forced vibration), the foundation global response was resonating with an excitation frequency of approximately 22–23 Hz. However, because the steady state operating frequency of the compressor was less than the foundation resonant frequency (13.1 versus 22–23 Hz), there was no global resonance of the soil-foundation system.
5. The maximum vertical and lateral response of the foundation was 0.36 mm (0.014 in.) and 0.91 mm (0.036 in.), respectively. Therefore, the foundation was classified as falling within the *very good* operational limit in accordance to Figure 3.10 of ACI 351 (ACI Committee 351 2004). This classification may lead to some notable vibrations in the foundation.

Pract. Period. Struct. Des. Constr., 2018, 23(3): 05018002

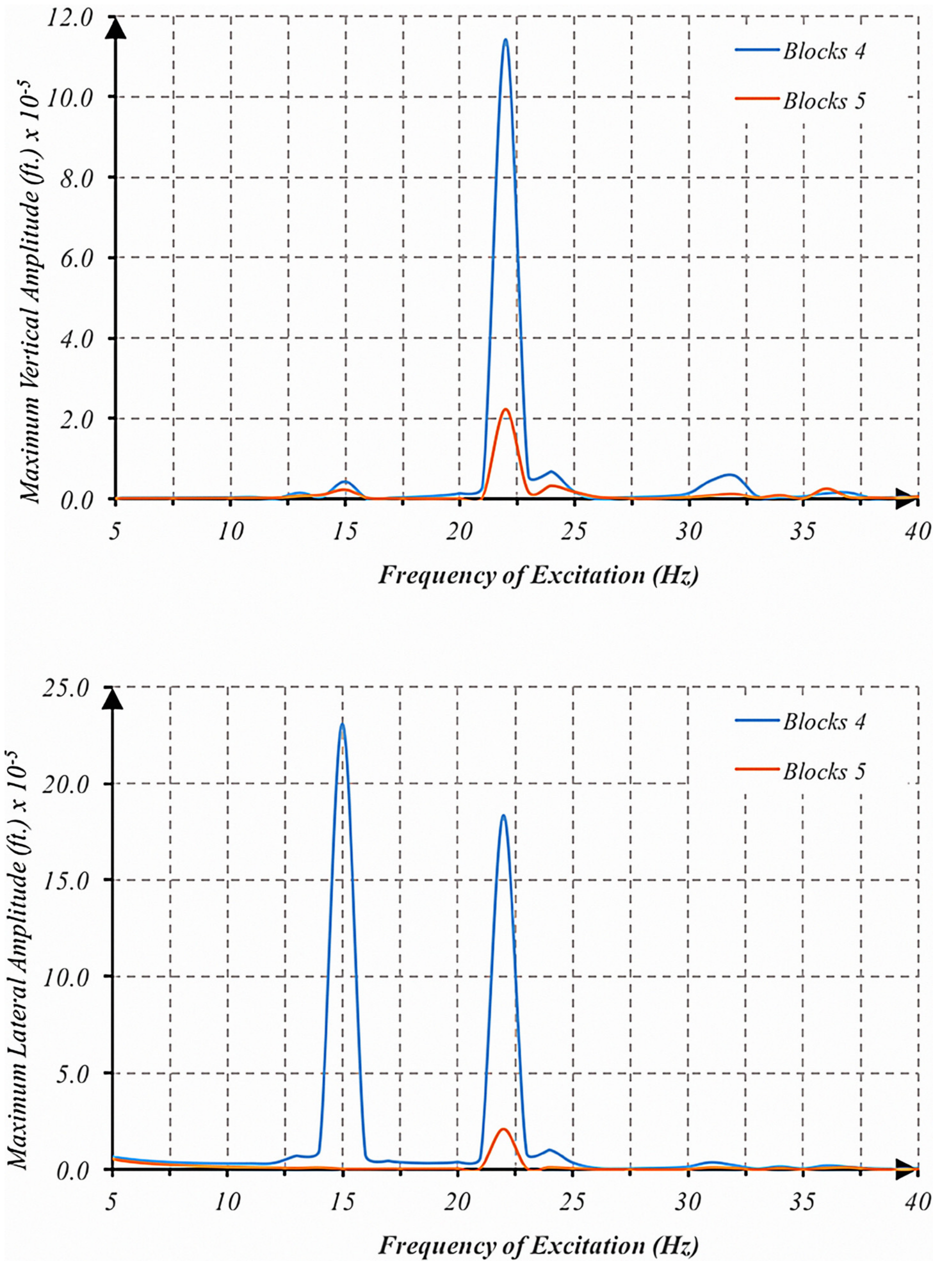

Fig. 13. Harmonic response of suction filter Supports 4 and 5

6. The classification of the foundation dynamic operational performance was considered *very good* [ACI 351, Figure 3.10 (ACI Committee 351 2004)] with an amplitude limit of 4.0 mm (0.156 in.); hence, notable vibrations were induced. These vibrations increased foundation fatigue, causing the machine to wear down more quickly than it would have otherwise and adversely reducing the foundation service-life limit. According to ACI 351, for machines to run smoothly, the foundation operational limit should be classified in the *very smooth* operational limit range (ACI Committee 351 2004). Therefore, to enhance the dynamic performance of the foundation so it falls under the very smooth operation category, it is the recommended that the lateral response of the individual suction filter support and discharge bottles support be reduced, which can be achieved by
   - Connecting the suction filter support piers and discharge bottles support piers monolithically to the cylinder support piers, and
   - Increasing the thicknesses of the filter support and discharge bottles support piers to increase the stiffness and shift natural frequency of both to be greater than the compressor steady-state operation frequency.

References

ACI (American Concrete Institute). (2011). *ACI 318-11: Building code requirements for structural concrete and commentary*, Farmington Hill, MI.

ACI Committee 351 (American Concrete Institute Committee 351). (2004). "Foundations for dynamic equipment." *ACI 351.34-04*, Farmington Hill, MI.

ANSYS 13 [Computer program]. ANSYS, Canonsburg, PA.

Arya, S., O'Neill, M., and Pincus, G. (1984). *Design of structures and foundations for vibrating machines*, Gulf, Houston, TX.

Chae, Y. S. (1969). “Vibration of noncircular foundations.” *J. Soil Mech. and Found. Div.*, 95(6), 1411–1430.

Kavvads, M., and Gazetas, G. (1993). “Kinematic seismic response and bending of free-head piles in layered soil.” *Géotechnique*, 43(2), 207–222.

Kobori, T. (1962). “Dynamical response of rectangular foundations on an elastic-space.” *Proc., Japan National Symp., Earthquake Engineering*, 81–86.

Lysmer, J., and Kuhlemeyer, R. L. (1969). “Finite dynamic model for infinite media.” *J. Engrg. Mech. Div.*, 95(4), 859–877.